Intelligent Interconnected Water Management System For Arid Zones Using Solar Photovoltaic Power

Kumarasaravanan K, Sridhar Ramasamy*, and Ilambirai RC

Department of Electrical and Electronics Engineering, SRM Institute of Science and Technology, Kattankulathur, Tamil Nadu 603203

* *Corresponding author. E-mail: sridharr@srmist.edu.in*

Received: Aug. 15, 2025; Accepted: Nov. 06, 2025

Effective water management schemes are needed to mitigate water scarcity issues in arid rural regions. Water distribution from a water resource to distant storage tanks often involves long conduit layouts with pumping motors, leading to pressure losses along the route. Powering and controlling these pumps become challenging when they are located in off-grid areas. This project proposes an Internet of Things (IoT)-enabled photovoltaic (PV) water pumping system with energy storage, suitable for regions where grid access is unavailable. The installed PV system charges the battery through a maximum power point tracking (MPPT) charge controller, and the stored energy is converted to AC using a sine pulse-width modulated (SPWM) inverter to drive the water pump. The system is emulated in MATLAB, and a hardware prototype has been developed using a 200 W PV module, charge controller, 12 V 100 Ah battery, TMS320F28379D-based SPWM inverter, ESP8266 IoT controller, and a 0.25 HP induction motor. The experimental results confirm that the coordinated MPPT–battery–SPWM inverter configuration maintains stable water flow and low total harmonic distortion (THD) even under fluctuating solar irradiance, while the IoT layer enables remote monitoring, automatic scheduling, and protection functions. These features collectively ensure reliable and energy-efficient water pumping, demonstrating that the proposed scheme offers a practical and intelligent solution for water transportation in arid rural areas.

Keywords: Photovoltaic; Water pumping; Internet of Things; Induction motor; MPPT; SPWM

http://dx.doi.org/10.6180/jase.202607_30.018

1. Introduction

According to global reports, though there is 60 % water on the planet, we only have about 3 % of it available for everyday use. People find it challenging to obtain water for household and agricultural needs, particularly in India, due to water scarcity. The expanding population is one of the primary causes of this scarcity, especially in rural areas where water cannot be wasted. Groundwater levels are declining because of urbanization, commercialization of agriculture following the Green Revolution, and heavy irrigation. People are affected by water scarcity in today's world since so many sectors require more water.

Proper water management is needed to utilize the available water rationally with minimal wastage. Due to climate change and inconsistent rainfall, the water demand in arid villages is further aggravated. The groundwater table has decreased, and pumping water from wells and underground sources has become very difficult [1, 2]. Agricultural production also takes a big hit in places where most of the yield depends on rainwater [3]. The transportation of water from available sources in arid regions is one of the solutions to mitigate water scarcity. This transportation is achieved through long conduit pipes from water resources to pumping or overhead tanks [4]. In this process, the water loses its pressure as it travels long distances within the con-

duits. To amplify the pressure, booster pumps are installed. These booster pumps maintain pressure and ensure proper water feed.

However, the biggest challenge here is providing an electric power source for the motors. In remote villages and hilly regions, there is no steady access to the utility grid. Moreover, the pipelines laid between villages may inherently pass through forest or hill regions, which are off-grid areas. In a PV water pumping system, the PV panels convert solar energy into electricity, which is then used to drive electric pumps. To power these motors, standalone PV panels with energy storage are a good solution. PV panel output varies with solar irradiation, and because of this, the water supply output also fluctuates. The introduction of a battery energy storage system solves not only the PV intermittency issue but also helps the pump operate during night hours [5].

The output characteristic curves of PV systems, namely I-V and P-V, vary with irradiation [6]. These curves exhibit a peak point at which the maximum power exists for a particular irradiance [7]. To ensure that this available peak power is extracted, intelligent power tracking schemes are used. These are called maximum power point trackers (MPPTs) [8]. Numerous MPPT schemes are available in literature [9, 10]. Each algorithm performs better than others from different perspectives. The most dominantly used algorithms are Incremental Conductance (INC), Perturb and Observe (P&O), Fractional Open-Circuit Voltage (OCV), and Short-Circuit Current (SCC). The OCV and SCC methods are not suitable in places where there are dynamic changes in irradiation and temperature [11]. The INC MPPT, on the other hand, is relatively complex in terms of coding due to its dependence on instantaneous and incremental conductance [12]. Hence, in most standalone applications, the P&O algorithm is the preferred MPPT scheme [13].

MPPT-based charging is more efficient than typical pulse width modulation (PWM) charging, as the current injection into the battery is relatively high [14]. The power electronic interfaces are selected according to the battery voltage and PV operating voltage. Buck, boost, or buck-boost converters are usually used between the PV and the battery, and the converter's duty cycle is derived from the MPPT algorithm [15]. The DC power from the battery is converted to AC voltage through an inverter. The choice of inverter depends on the capacity of the load. Water pumping is efficiently performed using AC motors, and the inverter is driven by a Sinusoidal Pulse Width Modulation (SPWM) scheme.

A square-wave inverter does not have the feature to control the output voltage, whereas in the SPWM scheme, by adjusting the modulation index, the output voltage can be controlled according to the desired value. In SPWM schemes such as unipolar and bipolar modulation, for instance, in a single-phase inverter, if bipolar switching is implemented, the output voltage switches between the positive and negative input voltage levels (+ Vdc and - Vdc). Here, a single sine wave is compared with a carrier signal to deliver control pulses. In the case of unipolar modulation, two sine waves are compared with a high-frequency triangular carrier, and output pulses are generated such that the voltage switches between +Vdc , zero, and -Vdc states. Due to reduced voltage stress, this scheme has lower switching losses and electromagnetic interference, resulting in a more efficient inverter drive [16]. The motor drive for pumping can be either an induction motor or a DC motor. Based on the application and the availability of converters and PWM control schemes, the appropriate motor drive can be selected [17, 18]. Remote control of the water pumping system becomes essential when the drive unit is located far away or in places where accessibility is difficult [19].

The Internet of Things (IoT) finds predominant applications in transport logistics and healthcare and is now expanding into energy and water systems. The IoT module is used to turn the motor on and off based on demand [20, 21]. In this work, the control aspects are enhanced by linking IoT with sensing circuits and additional parameters. The control parameters are tuned according to the specific response of the pumping motor based on feedback signals. This paper proposes an intelligent Internet of Things (IoT)-aided photovoltaic (PV)-fed water pumping system that addresses the issues of reliable pumping and remote control, as shown in Fig. 1.

The motor control is implemented through a Sinusoidal Pulse Width Modulated (SPWM) inverter, ensuring low Total Harmonic Distortion (THD) and high performance. The system is implemented in a simulation environment using MATLAB R2021 and in hardware using the TMS320F28379D controller for SPWM generation and ESP8266 for IoT control.

Existing PV-IoT-based water pumping systems reported in the literature primarily focus on basic automation or remote monitoring functions, often limited to ON/OFF motor control or simple data logging [9–13]. Many of these systems operate on direct PV coupling without intermediate energy storage, which restricts operation during low-irradiance or night-time conditions. In other implementations, square-wave or open-loop inverter drives are used, leading to high Total Harmonic Distortion (THD) and inefficient voltage regulation [14–16]. Further, IoT integration in

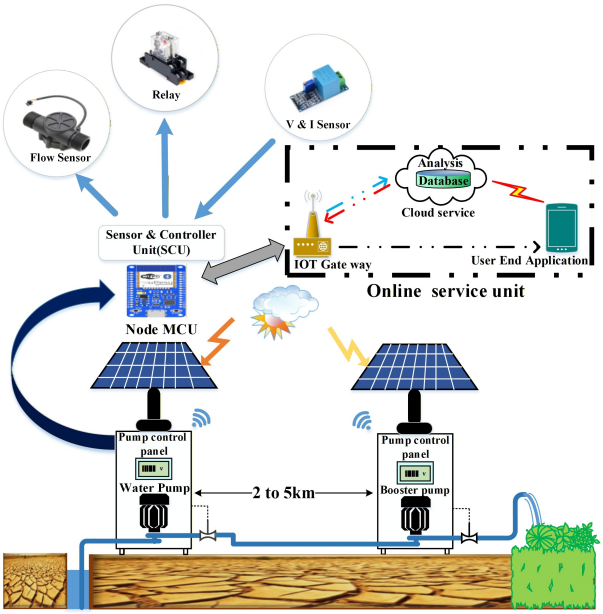

Fig. 1. Schematic diagram for IOT enabled Solar water pumping system

such systems is usually confined to status indication without any real-time coordination between the PV generation, energy storage, and motor control units.

In contrast, the proposed system introduces a coordinated PV-battery-SPWM inverter architecture with an IoT-enabled supervisory control layer. The MPPT-based charging unit maximizes PV utilization while maintaining optimum battery state-of-charge. The SPWM inverter, driven by a TMS320F28379D controller, ensures low-THD operation with adjustable modulation index for stable pump voltage and pressure regulation even under fluctuating irradiance. Additionally, the IoT layer (ESP8266) extends beyond simple motor switching-it provides intelligent feedbackbased monitoring, remote scheduling, and safety interlocks for pressure and flow variations. This integrated design enables continuous and reliable water pumping, including night-time operation, which is rarely addressed in earlier PV-IoT water pumping systems.

2. Methodology

2.1. IOT Enabled PV Water Pumping System

The overall system representation of the proposed work is shown in Fig. 2. In off-grid locations, the photovoltaic technique is more effective in resolving these issues. Because of unavailability of solar energy during the nights, lead acid batteries are used as backup supply in these schemes. A charge controller connects the PV and battery. The battery charges to 12 V, through the charge controller and feeds the inverter to achieve ac output of 14 V. A step up transformer boosts this voltage to $200 - 230$ V.

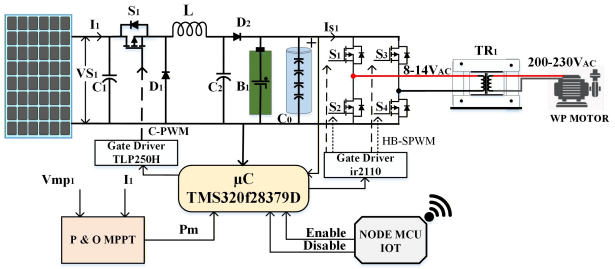

Fig. 2. System Architecture of IOT Enabled PV Water Pumping System

The ac output is fed to the water pump motor that operates at 230 V. Including an additional approach to the research paper, mobile application to access the motor via the Internet of Things is performed.

2.2. System Design and Specifications

The design specifications are worked for a distance of 5 km horizontally where the booster PV fed boost pumping is realized, for a 0.25 hp (horsepower) induction motor, which is equivalent to 186.5 W of power. The motor will be powered by a 12 V, 100Ah$LiFePO_4$ battery and charged by PV panels. IOT will control the motor to ensure efficient operation based on water demand and pressure. Water needs to be transported 5 km horizontally, which will require a pressure boosting design due to friction losses along the pipeline. For transporting water over 5 km , it is essential to consider pressure loss due to friction in the pipeline and any elevation changes.

The Darcy-Weisbach Equation helps estimate pressure loss due to friction in pipe:

$$\Delta \mathrm{Pf}\left(\frac{L}{D}\right) P_2^Z \tag{1}$$

Assume a typical pipe diameter of (0.1 m) and a velocity of 2 m/s, Friction factor for smooth pipes is around 0.02 for turbulent flow.

$$\Delta \mathrm{P} = 0.02 \times 50000 \times 2000 = 2,000,000$$

The most of the solar photovoltaic pump's system widely using centrifugal pumps. As rotodynamic pumps, they operate by imparting kinetic energy to water through a rapidly rotating impeller, which is then converted into pressure energy to push water through the pipeline. They are especially suited for solar-powered systems due to their simple construction, low maintenance, continuous and smooth flow characteristics, and compatibility with

variable power inputs. It is easy to couple with AC or DC motor. The power of hydraulic water pump is given by the following equation

$$P_{hyd(\text{ water })} = \rho \cdot g \cdot Q \cdot H \tag{2}$$

Were $\rho = 1000\ \text{kg}/m^3$, $\text{g} = 9.81, \text{H} = \text{total head (m)}$.

This is the estimated pressure loss due to friction. The pump must provide at least this amount of pressure to overcome friction, in addition to any required boost for delivery. Also, the flow rate requirement of 1 litre /sec is $\text{Q} = 1\ \text{L/s} = 0.001\ \text{m}^3/\text{s}$. The power required to overcome friction can be calculated using

$$\text{P}_{\text{friction}} = \text{Q} \cdot \Delta\text{P} = 2000\ \text{W} \tag{3}$$

the power shaft (pump)

$$P_{\text{shaft}} = \frac{P_{\text{hyd(water)}}}{\eta_{\text{pump (water)}}} \tag{4}$$

$\eta_{\text{pump (water)}}$ = pump efficiency ($0.65 - .085$),
Electrical power required to operate water pump

$$P_{\text{elec}} = \frac{P_{\text{shaft}}}{\eta_{\text{motor}}} \tag{5}$$

η_{motor} = efficiency of the motor
For the purpose of water transportation for long distance, series type boost pump is used, and the number of such identical pumps in series is given by

$$N_{\text{series}} = \left[\frac{H_{\text{reqried}}}{H_{\text{pump}}}\right] \tag{6}$$

The system needs to provide power for the motor and account for the duty cycle (how long the motor runs) and charge the battery for backup operation. The Volume delivered per day

$$V_{\text{day}} = \text{Q}\left(\frac{\text{L}}{\text{min}}\right) \times 60 \times sun\_hours/1000 \tag{7}$$

The paper also proposes a lab-scale experimental protocol and a field pilot configuration for validation. The power consumed by the 0.25 hp motor is $P_{\text{motor}} = 186.5$ W. The daily energy requirement is 746 Wh , for a typical motor that operates for about 4 hours in storage tank/arid location. The safety factor for system inefficiencies is 1.25. The average sunlight per day is evaluated for 6 hours.

To generate this energy, $\text{E}_{\text{PV}} = 746 \times 1.25 = 932.5$ Wh/ day

$$\begin{aligned} \text{E}_{\text{PV}_{\text{array}}} &= \frac{E_{PV}}{\text{system efficiency}} \\ &= \frac{932.5}{0.8} \\ &= 1165.6\ \text{Wh/ day} \\ P_{PV} &= \frac{1165.6}{6} \\ &= 194.27\ \text{W} \end{aligned} \tag{8}$$

Thus, the Eq. (8) The system need approximately a 200 W PV panel to meet the daily energy demand and charge the battery (assuming one day of autonomy) and for a battery depth of discharge of 80 %, the battery should store roughly 1, 165.6 Wh, which corresponds to a 12 V, 100Ah battery. This setup ensures that the motor can operate reliably even during periods of limited sunlight, providing a balanced and efficient solar-powered system.

2.3. PV Modeling and Sizing and P&O MPPT

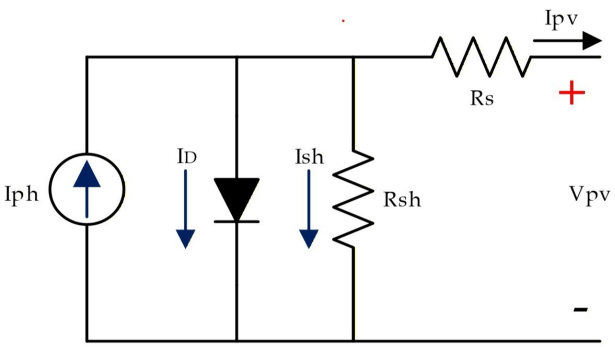

Fig. 3. Single Diode PV Cell Model

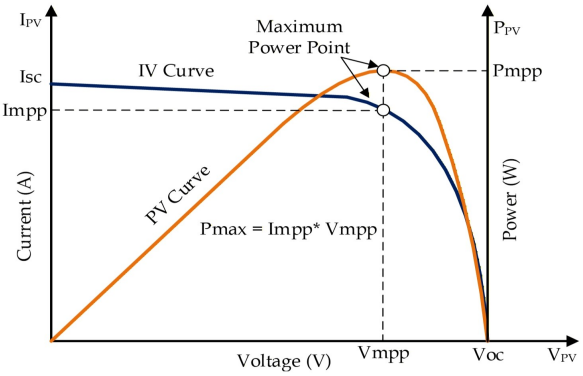

Fig. 4. P-V & I-V Curve

Fig. 3 shows the equivalent circuit of single cell PV model. PV cells are widely used and made of a variety of materials. At its most basic, PV cells work by converting solar energy into electronhole pairs, which subsequently separate and generate voltage in an external circuit. The magnitude of the irradiation falling on the panel is directly proportional to the photoelectric impact and the photovoltaic current expression is given by

$$I_{pv} = I_{ph} - I_o \left\{ \exp\left[\frac{V_{pv} + I_{pv}R_s}{N_s\left(\frac{\eta k_b T}{q}\right)}\right] - 1 \right\} - \frac{V_{pv} + I_{pv}R_s}{R_{sh}} \tag{9}$$

Table 1. Specifications of the PV source

S.No	Parameters	Ratings	Units
1	Maximum power (Pmax)	200	W
2	Maximum power voltage (Vmp)	36.1	Vdc
3	Maximum power current (Imp)	5.55	A
4	Open-Circuit voltage (Voc)	44.53	Vdc
5	Short-Circuit Current (Isc)	6	A
6	MPPT buck Converter	300	W

I_o is the saturation current of the diode, q is the electron charge ($1.602 \times 10 - 19C$), k is the Boltzmann constant ($1.3806503 \times 10 - 23\,J/K$) and T is the cell temperature. η is the ideality factor of an ideal diode. N_s is the number of cells arranged in series and N_p is the number of cells linked in parallel respectively. To compute the total current produced by PV module under partial shading effect 1 can be rewritten as in Eq. (3).

$$I_{pv} = N_p I_{ph} - I_o \left\{ \exp\left[\frac{V_{pv} + I_{pv} R_s \frac{N_s}{N_p}}{N_s \left(\frac{\eta k_b T}{q} \right)} \right] - 1 \right\} - \left\{ \frac{V_{pv} + I_{pv} R_s \frac{N_s}{N_p}}{\frac{N_s}{N_p} R_{sh}} \right\} \tag{10}$$

The I-V and P-V bends for different irradiance yet a settled temperature (25 °C) appeared in Fig. 4. The trademark I-V bend tells that there are two districts in the bend: one is the present source area and another is the voltage source locale.

In the voltage source district (in the correct side of the bend), the interior impedance is low and in the present source locale (in the left half of the bend), the impedance is high. Irradiance temperature assumes a vital part in anticipating the I-V trademark, and impacts of the two elements must be considered while plotting the PV system. Though the irradiance influences the yield, temperature chiefly influences the terminal voltage. The Perturb and Observe algorithm (P&O) is a broadly used MPPT algorithm in PV systems. The flow diagram presented in Fig. 5 presents the P&O algorithm where the operating point of the voltage is adjusted according to change in power. If the power increases, the operating point adjustment happens in the same direction and the direction is reversed if the value of the power decreases.

2.4. Sine Wave Bridge Inverter

A single-phase full bridge inverter is a circuit which converts a dc to single phase ac power with a single-phase output. sinusoidal pulse width modulated inverter converts DC voltage into AC voltage. The SPWM generation

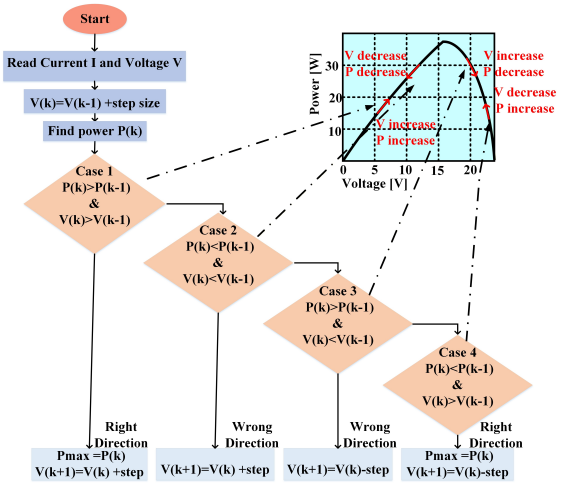

Fig. 5. P&O MPPT algorithm

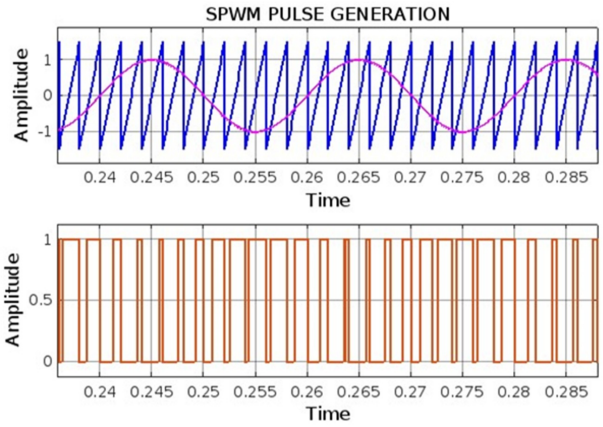

Fig. 6. SPWM -Pulse generator

ensures the inverter voltage free from harmonics as it generates pure sinewave output. A sinusoidal pulse width modulated inverter consists of several components, including an oscillator circuit, a comparator, a pulse generator, a filter circuit, and a power amplifier. The oscillator circuit generates a high-frequency square wave, which is then compared to a reference sine wave using the comparator. The SPWM generation is shown in Fig. 6. By controlling the duty cycle of the square wave, the effective voltage ap-

Table 2. Design Specifications of Battery, transformer and IM motor

S.No	Parameters	Ratings	Units
1	Battery ($LiFePO_4$	12 V, 100	Ah
2	Transformer turn ratio	(8V/220V) (27.5:1)	V_{rms}
3	maximum load in transformer	1	kVA
4	Water Pump induction motor	0.25	hp
5	Motor voltage and current	230, 2	V, A
6	Auxiliary (start)winding resistance and inductance	15,20	Ω, mH
7	Main winding resistance and inductance	10,50	Ω, mH
8	Maximum motor speed	2700	rpm

Table 3. Sensors and controllers

S.No	Parameters	Ratings	Units
1	Tms320f28379d	Upto200	MHz
2	Node MCU ESP8266	up to +19.5 dBm (802.11b), 2.4 to 2.4835(WI-FI)	dBm, GHz
3	Voltage Sensor LEM LV-25P	0-1000	V
4	Current Sensor LEM LA-55P	0-55	A
5	Water flow sensor	3/4 Inch Brass,1 Litres water = 477 pulse, accuracy: 10%	
6	Relays	12 V	V

Table 4. Comparison of water output with conventional and proposed IOT_solar water pumping system

Nominal Power (W)	Horse power (hp)	Litres per hour (conventional system) Total head H			Litres per hour (proposed system) Total head H		
		10 m	20 m	30 m	10 m	20 m	30 m
186.5	0.25	1666	834	500	1800	960	600
373	0.5	3334	1667	1000	3600	1800	1080
746	1	6667	3334	2,000	7200	3600	2100
1120	1.5	10,000	5,000	3,000	10,800	5400	3600

plied to the load can be regulated, resulting in a sine wave output.

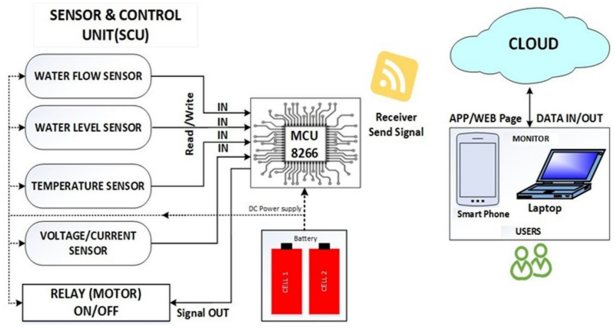

Fig. 7. Block diagram of Node MCU

2.5. IOT Control System

Fig. 7 illustrates a smart water management system using an ESP8266 Node MCU microcontroller as the central hub. The IOT controller, Node MCU (ESP8266), primarily serves as a central controller which coordinates with the multiple sensors, such as water flow sensor, water level sensor, temperature sensor, induction motor current and voltage sensors, motor's relay sensor and

Wi-Fi sensors, these sensors offer critical data for the controller which processes them and aid for the system's operation. The water level sensor in the storage tanks give information on the level of the water and ensures the motor operation on/off based on the cut off level both crest and trough. The water flow sensor ensures the effective water discharge in the conduit.

The pressure of the water needs to be maintained by the booster motor placed in equal intervals of the conduit. Similarly, the temperature and relay of motor are sensed. These data are accessible in a dash board or mobile application through an integration between internet and cloud storage, facilitates control and troubleshooting even from distant lo-

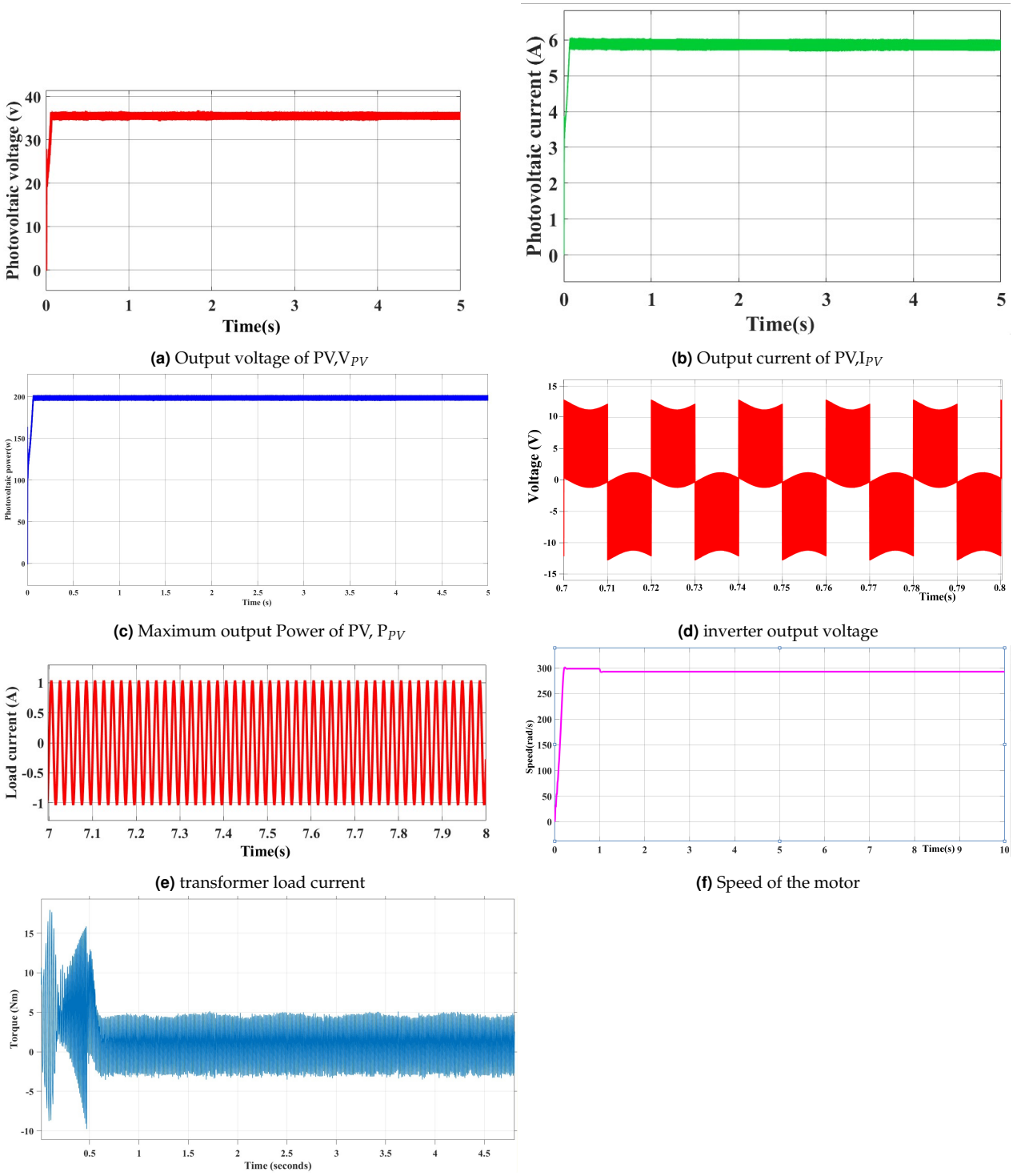

(a) Output voltage of PV,V_{PV}

(b) Output current of PV,I_{PV}

(c) Maximum output Power of PV, P_{PV}

(d) inverter output voltage

(e) transformer load current

(f) Speed of the motor

(g) Torque of the motor

Fig. 8. Simulation Results of PV fed IoT based water pumping system

cations. Even at places where human interventions are not possible this one-time enabled sensor - controller integrated system is completely an automated one.

3. Results and discussions

The 200 W PV system is designed to operate with an irradiance of 1000 W/m^2 and temperature of 25 °C under

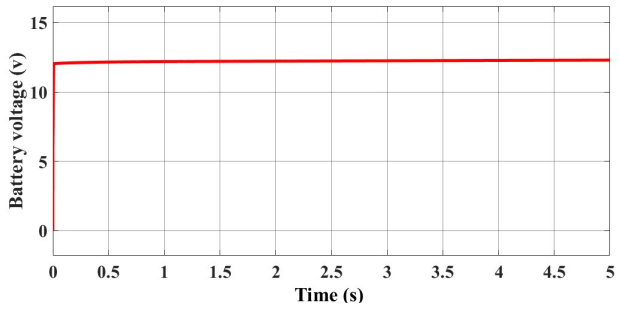

(a) Battery discharge voltage

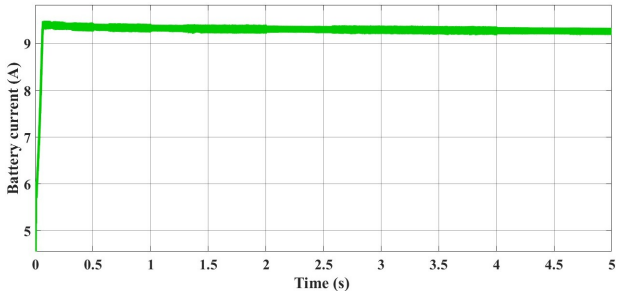

(b) Battery discharging Current

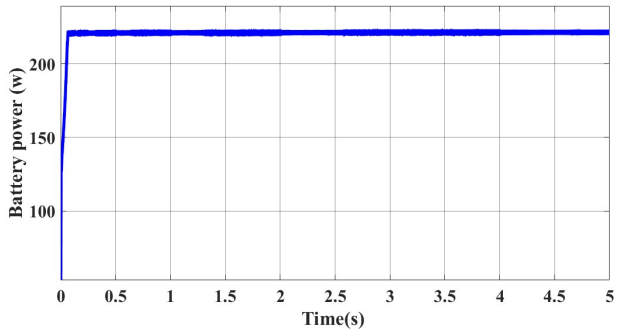

(c) Battery delivery power

Fig. 9. Simulation Results of Battery fed IoT based water pumping system

Standard Test Conditions (STC). As solar irradiance decreases, the power output proportionally declines as well. The charge controller regulates the PV input voltage by adjusting it to match the battery charging voltage. The pulses used in the H -bridge inverter have been generated by SPWM. The modulating signal is a sine wave, while the carrier signal is a triangular wave. The modulating frequency is 50 Hz, and the carrier frequency is 22 kHz. The load in this study is a singlephase induction motor with a nominal operating RMS voltage of 220 V. To meet this requirement, the inverter output must be stepped up using a transformer. The inverter's peak-to-peak voltage is 12 V, with an RMS voltage of 8 V. The voltage is stepped up from 8 V to 220 V where in the transformer is designed with a turn's ratio of $27.5 : 1 (8\,V/220\,V)$.

Tables 1 and 2 depicts the specifications of the PV panel and the battery, transformer and motor employed respectively.

The sensors, relays and controllers employed in this work is shown in Table 3.

The Average daily solar radiation of 7.15KWh/sq.m is radiant on the surface of PV array. The water output from conventional solar PV Water Pumping System is compared with the proposed IOT enabled PV water pumping system in Table 4. For the purpose of comparison, different dynamic heads are charted out in the table.

3.1. Simulation Results

The power conversion of photovoltaic (PV) input along with MPPT technique and also to charge the battery is implanted employing IOT. The transformer input is fed from the inverter and transmitted to the single-phase induction motor. MATLAB Simulink tool has been implemented to analyse the performance of the system. Standard Test Condition is performed at 1000 W/m^2 irradiation and 25°C. Fig. 8 shows the simulated results of the proposed PV aided water pumping system when PV alone is supplied to the system. The simulation results of the water pumping system are expressed in 3 different modes based on the input fed to the pumping system. They are as follows.

3.1.1. Case 1: When solar PV alone supplies the system:

When PV alone supplies, initially, there is a transient in the voltage and current and these curves maintains stability. Fig. 8a shows that PV voltage (V PV) in volts, and it shows an initial transient response before stabilizing at approximately 36 V. This stabilization occurs after a slight overshoot around 0.1 seconds, indicating that the system reaches a steady-state voltage level under the given conditions.

Fig. 8b shows the PV current IPV in amperes, which rises with a minor transient and then stabilizes around 0.8A. Both graphs indicate that the PV system successfully reaches a stable operating point, with minimal fluctuations after the initial transients, suggesting a stable load or well-regulated control in the system. The fast-settling time and smooth steady-state values imply efficient performance, potentially indicating a well-tuned maximum power point tracking (MPPT) mechanism.

In Fig. 8c the maximum output power of the PV obtained through along with time duration is illustrated. Fig. 8d inverter output voltage delivery to the input of transformer.

The simulated output speed curve of the motor and the torque of the motor are shown in Fig 8(g) and the speed of the motor initially increases to 300 rps and then stabilises at 290 rps.

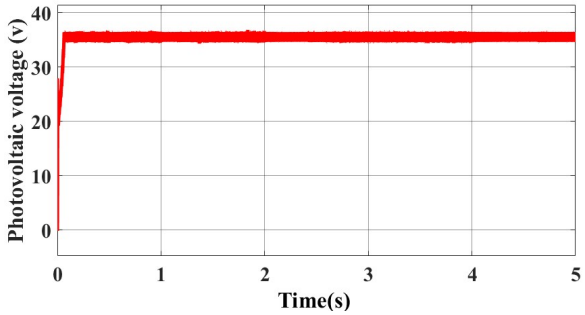

(a) Voltage delivered by PV

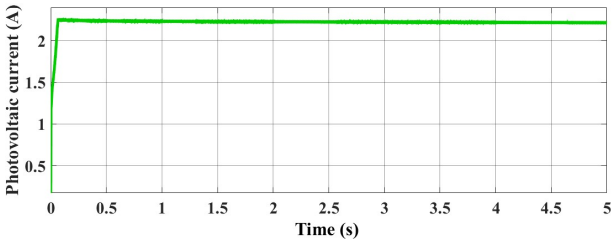

(b) Current delivered by PV

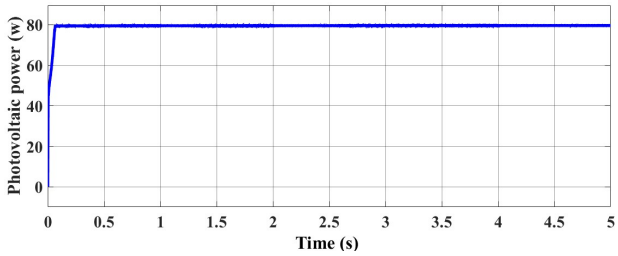

(c) Maximum Power of photovoltaic

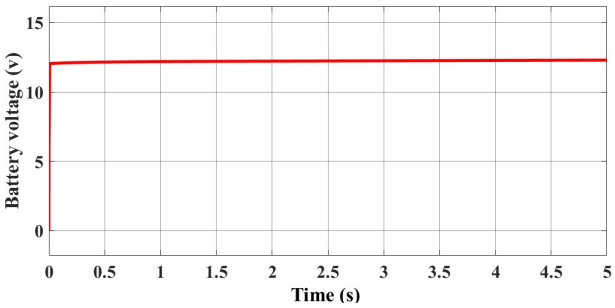

(d) Voltage delivered by battery

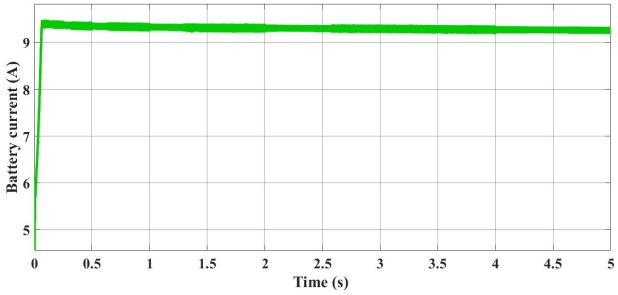

(e) Current delivered by battery

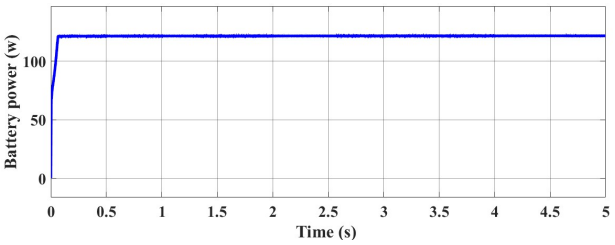

(f) Power delivered by the battery

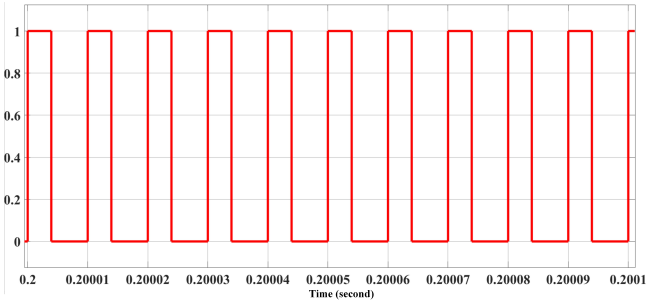

(g) MPPT Gate pulse

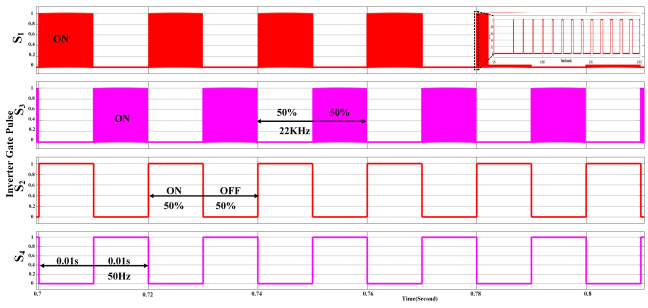

(h) MPPT Gate pulse

Fig. 10. Simulation Results of PV fed IoT based water pumping system

3.1.2. Case 2: When Battery alone supplies the system:

In this mode of operation, the battery alone supplies the water pumping system. This mode of operation is a standalone system where the battery is the only primary source that is supplying the system. As the battery keeps supplying the motor, the energy gets discharged and the battery voltage decreases.

Fig. 9a shows the simulated result of 12 V battery voltage that supplies the system and 18 A of discharging current is shown in Fig. 9b. In Fig. 9c, the power delivered by the battery is depicted.

3.1.3. Case 3: When both PV and Battery supplies the system

In this mode, both solar PV and battery is supplying the IOT enabled water pumping system, hence the system is

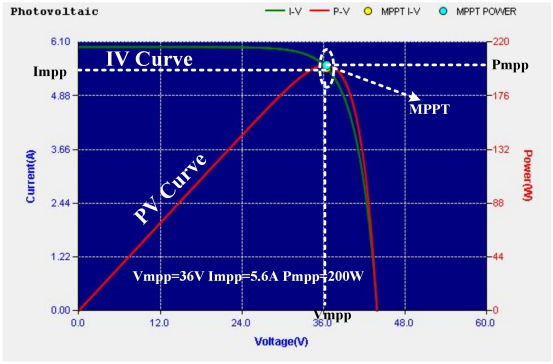

(a) Mppt 200 watts power delivered to load

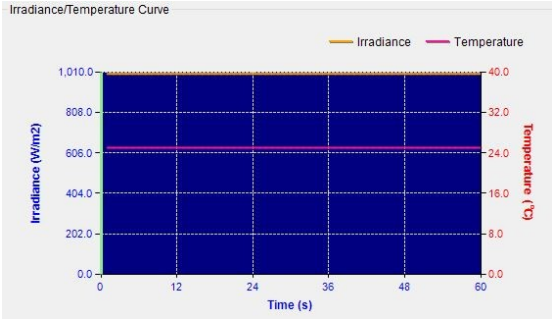

(b) 1000 W/m^2 irradiance & Temperature 25 °C

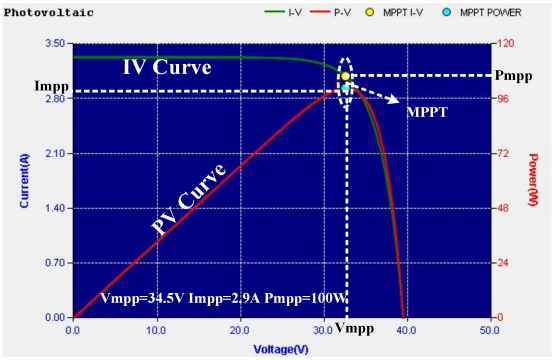

(c) Mppt 100 watts power delivered to load

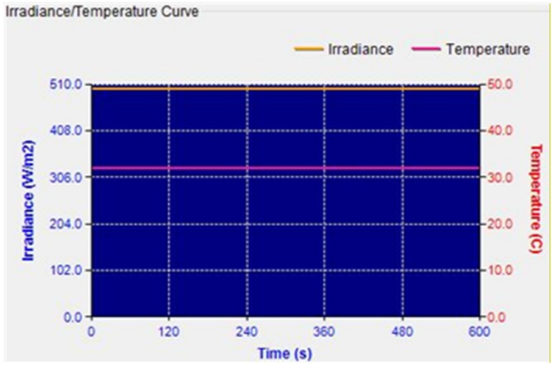

(d) 500 W/m^2 irradiance & Temperature 32 °C

Fig. 11. Simulation Results of PV fed IoT based water pumping system

now operating in hybrid mode.

Fig. 10b, the steady current profile indicates stable irradiance and temperature conditions, as well as effective operation of the maximum power point tracking (MPPT) control. The corresponding steady-state power output is approximately 80 W.

The current delivered by the battery is 9.5 A indicating the initial charging phase. In Fig. 10d, the voltage output of the battery remains constant at approximately. 12 V throughout, suggesting controlled voltage to prevent overcharging. Together, these indicate a standard constant current charging phase, typical in $LiFePO_4$ batteries, where current is held steady while voltage remains limited. In Fig. 10f, at the beginning there is a sharp increase in battery power, starting from nearly 0 W and quickly rising to a peak of around 150 W. This initial spike likely represents the inrush current or initial demand on the battery as it begins supplying power to the HBSPWM. Fig. 10g shows the SPWM generation in which a sine wave is compared with high frequency triangular wave. As a result of comparison between sine wave and high frequency triangular the PWM pulses are generated. In unipolar SPWM two reference pulses are acquired. The sine pulse is given to H-bridge that consists of 4 switches in which the diagonal switches are gives the same pulses. The steady oscillations after an initial period suggest that the motor has reached a stable operation, where the current is balanced with the load requirement. Fig. 10 shows the switching pulses fed to the inverter. Switches. The motor quickly accelerates to overcome the load's inertia and reach the pump's operating speed. After this, it settles into a steady speed, meaning the motor is efficiently matching the power needed to maintain a consistent water flow rate. Fig. 10h, the torque then decreases and stabilizes as the motor reaches a steady speed, requiring less torque to keep the pump running smoothly. This initial surge is typical in induction motor.

3.2. Field Testing and Experimental Results

The experimental setup uses a Waaree Energies WS-200/24V photovoltaic emulator module with a test value of 200 W under 1000 W/m^2 irradiance conditions. The Fig. 11a I-V and PV curves show the performance of the PV module. The MPPT was achieved at $V_{mpp} = 36$ V and $I_{mpp} = 5.6$ A, resulting in $P_{mpp} = 200$ W. This shows effective power extraction by the MPPT controller. The irradiance and temperature curve in Fig. 11b indicates constant environmental conditions at 1000 W/m^2 irradiance and 25°C temperature during the test. This ensures a stable performance analysis of the PV module and confirms the ability to maintain maximum output under steady condi-

tions.

Fig. 11c illustrates how the PV module performs when exposed to 500 W/m^2 of sunlight at a temperature of 32°C, delivering roughly 100 W. The I − V and P − V curves clearly highlight the maximum power point, which occurs at a voltage of about 34.5 V and a current of around 2.9 A. At this operating point, the MPPT controller fine-tunes the voltage and current so the panel consistently works at its highest possible efficiency.

Fig. 11d shows, the irradiance remains steady at 500 W/m^2 with the temperature fixed at 32 °C throughout the observation period, meanwhile the operating conditions are stable. Taken together, these plots demonstrate reliable MPPT action and steady power delivery from the PV system under the given environmental settings.

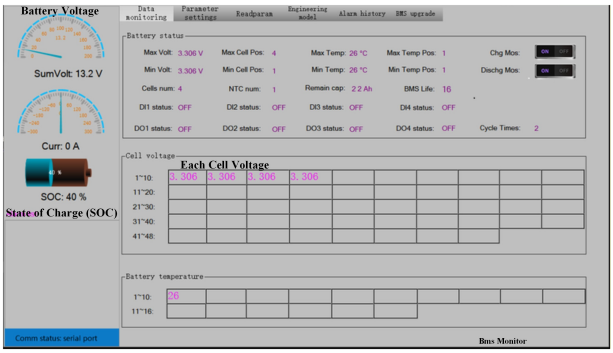

Fig. 12. BDaly BMS Battery SOC in PC

The Fig. 12 presents the BMS monitoring dashboard for the PV-powered, IoT-enabled water pumping setup. The interface provides live readings of the battery pack, including overall voltage, current flow, and state of charge. Each cell holds roughly 3.306 V, showing good balance across the four monitored cells. The system tracks battery temperature and recorded at 26 °C, while MOSFET switches handle both charging and discharging functions. The IoT setup supports remote supervision and control, ensuring the solar-driven pump operates safely, reliably, and at peak efficiency.

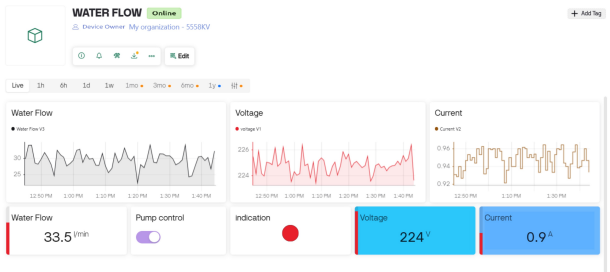

Fig. 13. IOT platform in Blynk Application

The Fig. 13, represents an IoT-based water flow monitoring system created using the Blynk application. It displays real-time data of water flow, voltage, and current. The Water Flow section shows live readings and a graphical trend of water flow rate in litres per minute. The Voltage and Current sensors monitor the electrical parameters of the pump. The Pump Control toggle allows remote operation of the pump, while the Indication light shows its status. The dashboard continuously updates, providing real-time monitoring, analysis, and control through the Blynk cloud platform, ensuring efficient water management and system performance tracking.

The Fig. 14 shows the photograph of the hardware prototype. The laboratory test setup essentially consists of a 12 V, 40 Ah $LiFePO_4$ battery, Tms320f28379d sine PWM generator PCB fabricator H-bridge inverter, a PWM charge controller, water pumping system and IOT device enabled by a mobile application. In order to expand the anti-interference capability, Tms320f28379d Inverter driver board has cross-conduction avoidance logic along with an LCD display interface which is helps the users to use the built-in display function. It is made up of two chips: Tms320f28379d control chip and the IR2110S driver chip.

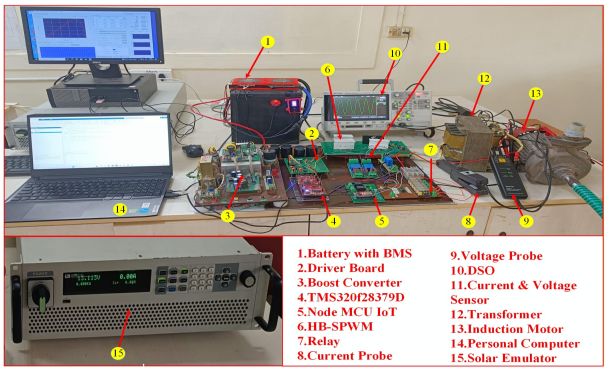

Fig. 14. Hardware Prototype

The ESP8266 is a compact Wi-Fi-enabled microcontroller that allows sensors and devices to be connected to the internet for remote operation. IoT applications involves a few straightforward steps to setup. Start by choosing a suitable ESP8266 development board common options include the NodeMCU and ESP-01. Next, configure the Arduino IDE so it can compile and upload programs to the module. Once the environment is ready, use code to link the ESP8266 to the local Wi-Fi network. You can then hook up the required hardware LEDs, relays, or various sensors to the GPIO pins and write the necessary control logic. After uploading the program to the board, the devices can be monitored and controlled online. Since the module operates over the

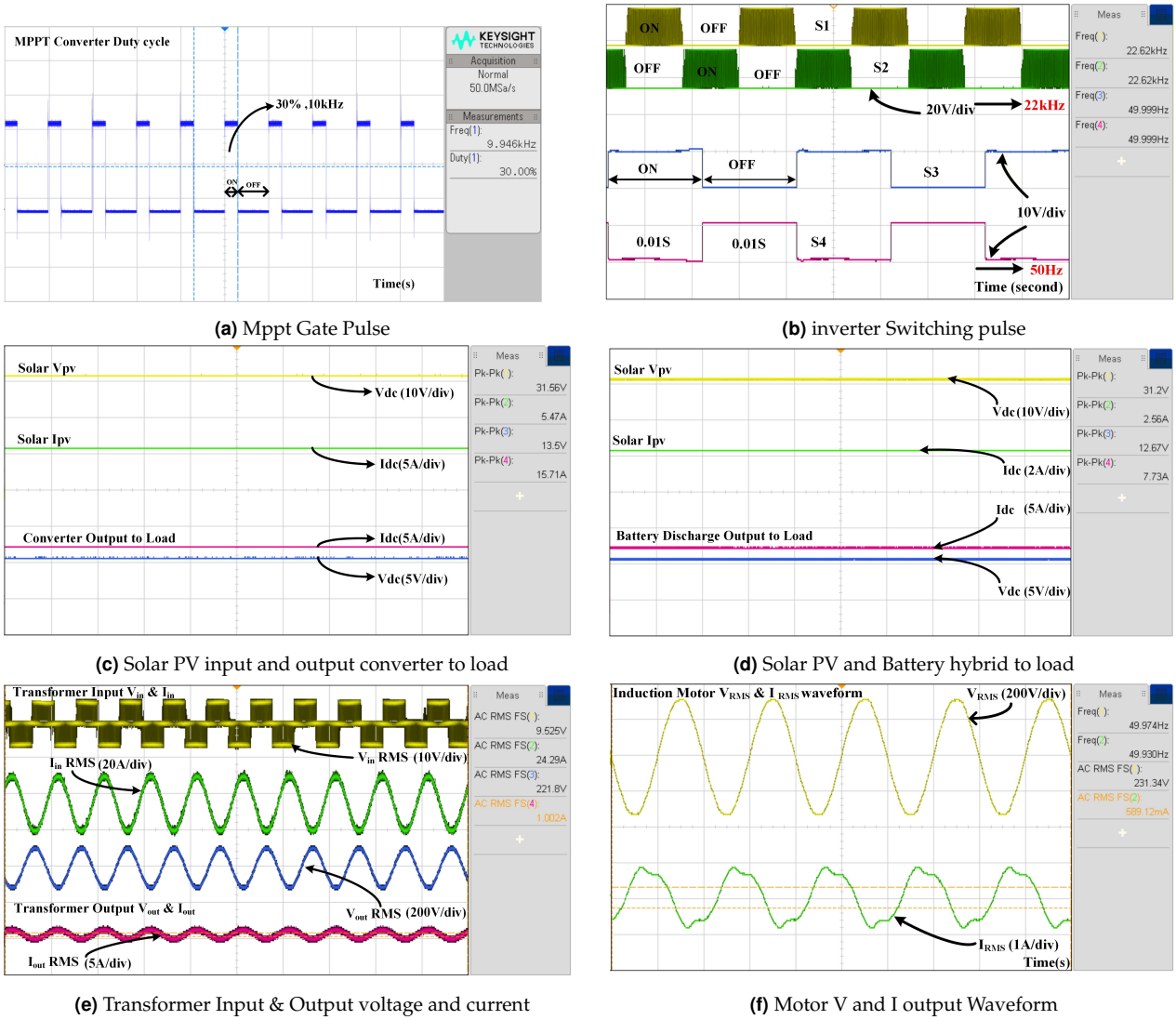

(a) Mppt Gate Pulse

(b) inverter Switching pulse

(c) Solar PV input and output converter to load

(d) Solar PV and Battery hybrid to load

(e) Transformer Input & Output voltage and current

(f) Motor V and I output Waveform

Fig. 15. Experimental results

internet, it's essential to use secure Wi-Fi, enable proper authentication and encryption, and validate inputs to safeguard the system from potential threats. A single-phase transformer is used when the supply voltage needs to be stepped up. In this case, raising the voltage from 8 V to 220 V calls for a turns ratio of about 27.5, obtained by dividing the secondary voltage by the primary voltage. This type of transformer simply transfers electrical energy between two circuits through electromagnetic induction.

An induction motor is typically used as the pump which operates on AC power and creates a rotating magnetic field in the stator windings. This rotating field induces current in the rotor, and the interaction between the stator and rotor magnetic fields produces the torque. Accordingly, the rotor drives the pump. Induction motors are widely favoured in pumping systems because they are durable, efficient, low-maintenance, and generally more economical than many alternative motor types. That said, choosing the right motor rating and design for the specific pump load is essential for proper performance and long-term reliability.

3.3. Hardware Results

The hardware experimental results, such as PWM pulses, output voltage of SPWM inverter and the inverter output after filtering, have been observed from DSO and shown in Fig. 15.

In Fig. 15a, the MPPT gate pulse operates at a frequency of 10 kHz with a 30 % duty cycle, indicating the converter's switching pattern used to track the MPP of the solar panel. This pulse controls the ON and OFF states of controller to regulate the duty ratio and optimize power extraction from the PV source. Fig. 15b shows the inverter switching pulses

corresponding to switches S1-S4, operating at 22 kHz carrier frequency and 50 Hz fundamental frequency with ON and OFF times of 0.01 s. These SPWM signals generate a sinusoidal AC output from the DC source, forming the basis of efficient DC-AC conversion.

Figs. 15c and 15d illustrate the behavior of the solar PV system and its converter under two operating conditions. In Fig. 15c, the load is supplied solely by the PV array. The solar voltage of about 31.56 V, current of 5.47 A, and the converter's output of 13.5 V and 15.71 A remain steady, showing that the system is transferring power efficiently.

Fig. 15d shows the hybrid operating mode, where the battery works alongside the PV panel to meet the load requirement. When the sunlight level drops and the PV output decreases, the battery steps in to support the system, ensuring uninterrupted power delivery. Under this mode, the battery contributes an output of roughly 12.67 V and 7.73 A.

The hardware results in Figs. 15e and 15f highlight how the transformer and induction motor behave within the solar PV-based power conversion setup. Fig. 15e shows the input and output waveforms of the transformer as captured on the DSO. The input side displays pulsed voltage and current signals-typical of an inverter-fed transformer-while the output waveforms appear smoother, indicating proper filtering and effective AC conversion. The measured RMS values confirm that the transformer steps up the voltage as intended and supplies the necessary current for the AC load.

Fig. 15f presents the voltage and current waveforms of the induction motor. The transformer, driven by the inverter, delivers a near-sinusoidal voltage of about 231 V RMS along with the corresponding motor current. As expected for an inductive load, the current waveform shows a slight phase lag behind the voltage. These observations verify that both the inverter and transformer are operating correctly, ensuring stable AC output. Overall, the results demonstrate efficient voltage transformation, reliable energy transfer, and the system's capability to run an AC induction motor using solar-derived DC power.

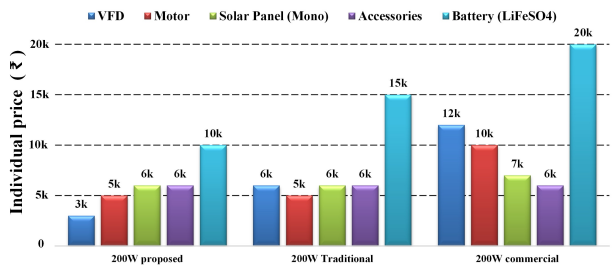

Fig. 16. Cost comparison

Fig. 16 shown the induvial material cost, the total system cost for the developed prototype (200 W PV capacity) is approximately ₹30,000 (INR), including the PV module (₹6,000), battery (₹10,000), 0.25 hp Monoblock water pump (₹5000), MPPT charge controller & inverter (VFD) (₹3000) with control board (₹4,000), and IoT along with sensing units (₹2,000). When scaled to a 1 kW system, the estimated cost per delivered watt is around ₹120-130/W, which is 25-30 % lower than comparable PV-pumping systems with grid-tied or variable-frequency drive (VFD) configurations. The low-cost ESP8266 controller and standalone SPWM inverter topology significantly reduce hardware complexity and recurring operational costs.

4. Conclusion

This work has proposed an IOT enabled PV module driven Induction motor water pumping system for water management in arid villages. The design considerations of the inverter drive, storage battery, and motor drive are duly investigated. The key advantages of the proposed system are:

1. IOT enabled control helps in accessing the motor parameters even at distance. The on/off control can be done through a mobile application.

2. The most reliable battery charging scheme is ensured through a P&O algorithm aided buck converter MPPT scheme.

3. The SPWM is developed through TMS320f28379D and the inverter module is made so compact that the switches are embedded within the drive unit.

4. Since the system is bestowed with remote control, simplicity, improved performance, and low cost, the IOT enabled PV fed induction motor drive will become ideal set up for distant controlled pumping.

5. Typical standard rule for 0.25 hp delivery flow water in minimum 3 kl/day.

6. Future work can focus on extending the present system towards higher-capacity PV arrays and multi-pump coordination for community-level water distribution. The integration of predictive analytics and AI-assisted IoT control could further enhance energy optimization, fault prediction, and autonomous scheduling based on weather and water demand data. Incorporating DC microgrid compatibility and hybrid renewable inputs (such as wind or small hydro) would also make the system more versatile and resilient for large-scale rural deployment.

5. Acknowledgement

The authors of this article gratefully acknowledge the Renewable Energy Research Laboratory (RERL) at SRM Institute of Science and Technology (SRMIST) for providing the infrastructure and support necessary to conduct this research. They also extend their gratitude to the Science and Engineering Research Board (SERB) for funding this work under the Teachers Associateship for Research Excellence (TARE) Scheme, Grant Number TAR/2022/000547.

nomenclature

Acronyms

ΔP	Pressure loss (Pa)
ρ	Density of water $(1000\ kg/m^3)$
ϑ	Velocity of water (m/s)
D	Diameter of the pipe (m)
f	Darcy friction factor (dimensionless, depends on pipe material and flow regime)
I_D	Diode current
I_{mp}	Current at maximum power point
I_o	Output current of photovoltaic
I_{ph}	Photo current
I_{pv}	Output current of the photovoltaic
I_{sc}	Short circuit current
I_{sh}	Shunt current
K_b	Boltzmann constant $(1.380653 \times 10^{-23}\ J/K)$
L	Length of the pipe (5,000 m)
MMPT	maximum power point tracking
N_p	number of cells connected in parallel η = Ideality factor
N_s	Number of cells connected in series)
$P_{friction}$	Friction power
P_{motor}	Power consumption of the motor
P_{pv}	Power of the Photovoltaic
q	Electron charge (1.602×10^{-19}C)
R_{sh}	Shunt Resistance
R_s	Series resistance
T	Temperature of the panel
V_{mp}	Voltage at maximum power point
V_{oc}	Open circuit voltage
V_{pv}	Output voltage of photovoltaic

References

[1] A. Boutelhig and Y. Bakelli. "Comparative study on Water Max A 64 DC pump performances based Photovoltaic Pumping System design to select the optimum heads in arid area". In: *2012 24th International Conference on Microelectronics (ICM)*. 2012, 1–5. DOI: 10.1109/ICM.2012.6471413.

[2] U. Kumari, K. Swamy, A. Gupta, R. R. Karri, and B. C. Meikap. "Chapter8 - Global water challenge and future perspective". In: *Green Technologies for the Defluoridation of Water*. Ed. by M. Hadi Dehghani, R. Karri, and E. Lima. Elsevier, 2021, 197–212. DOI: https://doi.org/10.1016/B978-0-323-85768-0.00002-6.

[3] G. D. Kamalapur and R. Y. Udaykumar. "Electrification in rural areas of India and consideration of SHS". In: *2010 5th International Conference on Industrial and Information Systems*. 2010, 596–601. DOI: 10.1109/ICIINFS.2010.5578635.

[4] G. Li, Y. Jin, M. Akram, and X. Chen, (2017) *"Research and current status of the solar photovoltaic water pumping system â€“ A review"* **Renewable and Sustainable Energy Reviews *79***(C): 440–458. DOI: 10.1016/j.rser.2017.05.055.

[5] R. Rajan, N. M. C. M, M. R. M. P, and J. P. "Battery Supported Solar PV-based PMSM Driven Water Pumping System". In: *2021 International Conference on Communication, Control and Information Sciences (ICCISc)*. ***1***. 2021, 1–6. DOI: 10.1109/ICCISc52257.2021.9484904.

[6] S. Pathy, C. Subramani, R. Sridhar, T. M. Thamizh Thentral, and S. Padmanaban, (2019) *"Nature-Inspired MPPT Algorithms for Partially Shaded PV Systems: A Comparative Study"* **Energies *12***(8): DOI: 10.3390/en12081451.

[7] A. Ballaji and R. Dash, (2023) *"A Comprehensive Review on Latest State of the Art Practices in MPPT Algorithm"* **Distributed Generation & Alternative Energy Journal *38***(03): 875–906. DOI: 10.13052/dgaej2156-3306.3837.

[8] M. A. Eltawil and Z. Zhao, (2013) *"MPPT techniques for photovoltaic applications"* **Renewable and Sustainable Energy Reviews *25***: 793–813. DOI: https://doi.org/10.1016/j.rser.2013.05.022.

[9] A. J. Alrubaie, A. Al-Khaykan, R. Q. Malik, S. H. Talib, M. I. Mousa, and A. M. Kadhim. "Review on MPPT Techniques in Solar System". In: *2022 8th International Engineering Conference on Sustainable Technology and Development (IEC)*. 2022, 123–128. DOI: 10.1109/IEC54822.2022.9807500.

[10] R. B. Bollipo, S. Mikkili, and P. K. Bonthagorla, (2021) *"Hybrid, optimal, intelligent and classical PV MPPT techniques: A review"* **CSEE Journal of Power and Energy Systems *7***(1): 9–33. DOI: 10.17775/CSEEJPES.2019.02720.

[11] S. Motahhir, A. El Hammoumi, and A. El Ghzizal, (2020) *"The most used MPPT algorithms: Review and the suitable low-cost embedded board for each algorithm"* **Journal of Cleaner Production *246***: 118983. DOI: https://doi.org/10.1016/j.jclepro.2019.118983.

[12] M. A. Elgendy, B. Zahawi, and D. J. Atkinson, (2015) *"Operating Characteristics of the P&O Algorithm at High Perturbation Frequencies for Standalone PV Systems"* **IEEE Transactions on Energy Conversion *30***(1): 189–198. DOI: 10.1109/TEC.2014.2331391.

[13] M. Kermadi, Z. Salam, A. M. Eltamaly, J. Ahmed, S. Mekhilef, C. Larbes, and E. M. Berkouk, (2020) *"Recent developments of MPPT techniques for PV systems under partial shading conditions: a critical review and performance evaluation"* **IET Renewable Power Generation *14***(17): 3401–3417.

[14] P. K. Atri, P. S. Modi, and N. S. Gujar. "Design and Development of Solar Charge Controller by Implementing two different MPPT Algorithm". In: *2021 International Conference on Advances in Electrical, Computing, Communication and Sustainable Technologies (ICAECT)*. 2021, 1–5. DOI: 10.1109/ICAECT49130.2021.9392426.

[15] H. Zhu, D. Zhang, H. S. Athab, B. Wu, and Y. Gu, (2015) *"PV Isolated Three-Port Converter and Energy-Balancing Control Method for PV-Battery Power Supply Applications"* **IEEE Transactions on Industrial Electronics *62***(6): 3595–3606. DOI: 10.1109/TIE.2014.2378752.

[16] K. Taniguchi, Y. Ogino, and H. Irie, (1988) *"PWM technique for power MOSFET inverter"* **IEEE Transactions on Power Electronics *3***: 328–334.

[17] A. K. Mishra, B. Singh, and T. Kim, (2023) *"An Economical Solar Water Pump With Grid and Battery Backup for Continuous Operation"* **IEEE Journal of Emerging and Selected Topics in Industrial Electronics *4***(1): 109–117. DOI: 10.1109/JESTIE.2022.3192212.

[18] S. Shukla, B. Singh, P. Shaw, A. Al-Durra, T. H. M. El-Fouly, and E. F. El-Saadany, (2022) *"A New Analytical MPPT-Based Induction Motor Drive for Solar PV Water Pumping System With Battery Backup"* **IEEE Transactions on Industrial Electronics *69***(6): 5768–5781. DOI: 10.1109/TIE.2021.3091929.

[19] J. Meyer and S. von Solms, (2018) *"Solar Powered Water Security: An Enabler for Rural Development in Limpopo South Africa"* **IEEE Access *6***: 20694–20703. DOI: 10.1109/ACCESS.2018.2805367.

[20] P. Jaya Prakash Reddy, G. Viswanadh, and S. Kumar Singh. "IOT based Smart Water Pump Switch". In: *2021 2nd International Conference on Intelligent Engineering and Management (ICIEM)*. 2021, 534–538. DOI: 10.1109/ICIEM51511.2021.9445278.

[21] B. H. Naveen, H. R. Sridevi, and S. V. Kulkarni. "IoT-Enabled Solar-Powered Intelligent Agriculture System". In: *2022 IEEE 2nd Mysore Sub Section International Conference (MysuruCon)*. 2022, 1–6. DOI: 10.1109/MysuruCon55714.2022.9972656.